

AD

TECHNICAL REPORT ARCCB-TR-98006

**COMPRESSIVE THERMAL YIELDING LEADING
TO HYDROGEN CRACKING IN A FIRED CANNON**

**JOHN H. UNDERWOOD
ANTHONY P. PARKER
PAUL J. COTE
SAMUEL SOPOK**

APRIL 1998



**US ARMY ARMAMENT RESEARCH,
DEVELOPMENT AND ENGINEERING CENTER
CLOSE COMBAT ARMAMENTS CENTER
BENÉT LABORATORIES
WATERVLIET, N.Y. 12189-4050**



APPROVED FOR PUBLIC RELEASE; DISTRIBUTION UNLIMITED

DTIC QUALITY INSPECTED 41

19980521 003

DISCLAIMER

The findings in this report are not to be construed as an official Department of the Army position unless so designated by other authorized documents.

The use of trade name(s) and/or manufacturer(s) does not constitute an official indorsement or approval.

DESTRUCTION NOTICE

For classified documents, follow the procedures in DoD 5200.22-M, Industrial Security Manual, Section II-19 or DoD 5200.1-R, Information Security Program Regulation, Chapter IX.

For unclassified, limited documents, destroy by any method that will prevent disclosure of contents or reconstruction of the document.

For unclassified, unlimited documents, destroy when the report is no longer needed. Do not return it to the originator.

REPORT DOCUMENTATION PAGE

Form Approved
OMB No. 0747-0188

This report contains information that is not to be disseminated outside the agency or its contractors, including the information contained in this report, unless specifically authorized by the agency. If you are a contractor, you are to disseminate this information only to those personnel who have a valid need to know. Send comments regarding this report to the Office of Management and Support, Paperwork Reduction Project (0747-0188), Washington, DC 20301.

1. AGENCY USE ONLY (Leave blank) 2. REPORT DATE
April 1998 3. REPORT TYPE AND DATES COVERED
Final

4. TITLE AND SUBTITLE
COMPRESSIVE THERMAL YIELDING LEADING TO HYDROGEN CRACKING IN A FIRED CANNON

5. AUTHOR(s)
John H. Underwood, Anthony P. Parker (Royal Military College of Science, Cranfield University, UK), Paul J. Cote, and Samuel Sopok

6. AUTHORING ORGANIZATION NAME(S) AND ADDRESS(ES)
U.S. Army ARDEC
Benet Laboratories, AMSTA-AR-CCB-O
Watervliet, NY 12189-4050

7. PERFORMING ORGANIZATION NAME(S) AND ADDRESS(ES)
U.S. Army ARDEC
Close Combat Armaments Center
Picatinny Arsenal, NJ 07806-5000

8. PERFORMING ORGANIZATION REPORT NUMBER
ARCCB-TR-98006

9. PROGRAM ELEMENT, PROJECT, TASK NUMBER AND REPORT NUMBER
AMCMS No. 6226.24.H180.0
PRON No. TU6A6F361ABJ

To be presented at the ASME Pressure Vessels and Piping Conference, San Diego, CA, 26-30 July 1998.
To be published in *ASME Journal of Pressure Vessel Technology*.

Approved for public release; distribution unlimited.

Investigation of environmental cracking of a 1100 MPa yield strength A723 steel cannon tube subjected to prototype firings is described. Metallographic results show cracking of the steel beneath a 0.12 mm protective layer of chromium. Cracks undermine and remove sections of chromium and lead to localized erosion that ruins the cannon. Key features of the firing thermal damage and cracking are: [i] recrystallization of the chromium to a depth of up to 0.08 mm; [ii] steel transformation to 0.19 mm below the chrome surface; [iii] two different periodic arrays of cracks normal to the hoop and axial directions, with mean depths of 0.23 and 0.46 mm, respectively.

Time-temperature-depth profiles for the firing cycle were derived via bi-material finite difference analysis of a semi-infinite solid which incorporated cannon combustion gas temperatures and material properties that vary as a function of temperature. The temperature and depth associated with the steel transformation were used to solve iteratively for the convective heat transfer coefficient. This value was further confirmed by the depths of chromium recrystallization and of the crack arrays in the two orientations. A profile of maximum temperature versus depth is used to determine the near-bore applied and residual stress distributions within the tube. The measured volume change of steel transformation is used to determine an upper limit on applied and residual stresses. These stresses are used to determine crack-tip stress intensity factors for the observed crack arrays and hence provide some explanation for the differential depths of cracking.

The near-bore temperature and residual stress distributions are used to help determine the cause of hydrogen cracking and measures to prevent cracking. Compressive yielding due to thermal loading produces near-bore tensile residual stresses and thereby causes hydrogen cracking. Prevention of cracking is discussed in relationship to hydrogen crack growth rate tests of alternative alloys and coatings.

Thermal Yielding, Environmental Cracking, Hydrogen Cracking, A723 Steel, Cannon Tubes, Residual Stress, Stress Intensity Factors 10

UNCLASSIFIED UNCLASSIFIED UNCLASSIFIED UL

TABLE OF CONTENTS

| | <u>Page</u> |
|--|-------------|
| ABSTRACT | 1 |
| INTRODUCTION | 1 |
| NOMENCLATURE | 1 |
| OBSERVATIONS | 2 |
| NEAR-BORE TEMPERATURES | 2 |
| NEAR-BORE THERMAL EXPANSION AND PHASE-CHANGE EFFECTS | 4 |
| NEAR-BORE STRESSES | 5 |
| SUMMARY AND CONCLUSIONS | 8 |
| ACKNOWLEDGEMENTS | 9 |
| REFERENCES | 9 |

TABLES

| | |
|---|---|
| 1. Observations from Metallographic Sections of a Fired Cannon | 2 |
| 2. Thermal Properties of Metallic Materials Used in Finite Difference Procedure | 4 |

LIST OF ILLUSTRATIONS

| | |
|--|---|
| 1. Polished and Etched Sections from Near-Bore Region of a Cannon Following Forty Prototype Firings, 100X; (a) section showing C-R cracks, the steel microstructure and microhardness indentations; (b) section showing L-R cracks and the chromium microstructure | 3 |
| 2. Polished and Etched Sections from Near-Bore Region of a Cannon Following Forty Prototype Firings, 100X; section showing C-R cracks, the steel microstructure and the start of rapid erosion | 3 |
| 3. Semi-Infinite Plate Representation and Location of Finite Difference Nodes | 4 |
| 4. Finite Difference Temperature-Time-Depth Profile Based Upon Known Depth of Transformation | 6 |
| 5. Finite Difference Maximum Temperature versus Depth for $h = 198,000 \text{ W/m}^2\cdot\text{K}$ | 6 |
| 6. Dilation Behavior of a Low Alloy Steel as a Function of Temperature | 7 |
| 7. Near-Bore Residual Stresses After Heating and Cooling | 7 |
| 8. Stress Intensity Factors for C-R and L-R Cracks Based Upon Observed Crack Spacing | 8 |

COMPRESSIVE THERMAL YIELDING LEADING TO HYDROGEN CRACKING IN A FIRED CANNON

John H. Underwood
US Army Armament Research
Development and Engineering Center
Benet Laboratories, Watervliet, NY

Anthony P. Parker
Royal Military College of Science
Cranfield University
Swindon, England

Paul J. Cote
US Army Armament Research
Development and Engineering Center
Benet Laboratories, Watervliet, NY

Samuel Sopok
US Army Armament Research
Development and Engineering Center
Benet Laboratories, Watervliet, NY

ABSTRACT

Investigation of environmental cracking of a 1100 MPa yield strength A723 steel cannon tube subjected to prototype firings is described. Metallographic results show cracking of the steel beneath a 0.12 mm protective layer of chromium. Cracks undermine and remove sections of chromium and lead to localized erosion that ruins the cannon. Key features of the firing thermal damage and cracking are:

- [i] recrystallization of the chromium to a depth of up to 0.08 mm;
- [ii] steel transformation to 0.19 mm below the chrome surface;
- [iii] two different periodic arrays of cracks normal to the hoop and axial directions, with mean depths of 0.23 and 0.46 mm, respectively.

Time-temperature-depth profiles for the firing cycle were derived via bi-material finite difference analysis of a semi-infinite solid which incorporated cannon combustion gas temperatures and material properties that vary as a function of temperature. The temperature and depth associated with the steel transformation were used to solve iteratively for the convective heat transfer coefficient. This value was further confirmed by the depths of chromium recrystallization and of the crack arrays in the two orientations. A profile of maximum temperature versus depth is used to determine the near-bore applied and residual stress distributions within the tube. The measured volume change of steel transformation is used to determine an upper limit on applied and residual stresses. These stresses are used to determine crack-tip stress intensity factors for the observed crack arrays and hence provide some explanation for the differential depths of cracking.

The near-bore temperature and residual stress distributions are used to help determine the cause of hydrogen cracking and measures to prevent cracking. Compressive yielding due to thermal loading produces near-bore tensile residual stresses and thereby causes hydrogen cracking. Prevention of cracking is discussed in relationship to hydrogen crack growth rate tests of alternative alloys and coatings.

INTRODUCTION

There is always interest in increasing the firing pressure of a cannon, in order to produce higher projectile velocity and range. The higher

pressure is naturally accompanied by higher temperature, which causes increased problems with cannon tube materials. This progression of problems related to increasing cannon firing pressure and temperature is the general topic of this paper. The specific example problem discussed here arose from the prototype firing of a cannon with the high firing pressure typical of modern cannon, (Underwood and Parker, 1995), but with an unusually high propellant gas temperature which caused unexpectedly severe problems with the cannon tube bore surface. The cannon firing conditions will be described, within proprietary limits, and the cannon material degradation will be used to guide an investigation of temperature and stress distributions and associated arrays of cracks observed in the near-bore region of the cannon tube. In complementary work to this paper (Parker, 1998) one of the present authors proposes a model that relates edge-crack depth to crack spacing in a variety of physical situations which involve a relatively thin surface layer containing tensile residual stress. This model will be used in this current work to describe the important depth and spacing of crack arrays in metal surfaces exposed to the high cannon firing temperatures.

NOMENCLATURE

| | |
|------------|--|
| c_p | specific heat at constant pressure (J/kg.K) |
| d | distance between edge cracks |
| E | Young's modulus |
| h | convection heat transfer coefficient (W/m ² .K) |
| K | crack tip stress intensity factor (MPa ^{1/2}) |
| k | thermal conductivity (W/m.K) |
| T | absolute temperature (K) |
| t | time (secs) |
| x | distance from free surface (mm) |
| α | thermal diffusivity (m ² /sec) |
| α^* | coefficient of thermal expansion (m/m.K) |
| ν | Poisson's ratio |
| σ | direct stress (MPa) |

OBSERVATIONS

The cannon tube that experienced problems due to high firing temperatures was the same type as that described in Underwood and Parker (1995). It has an inner radius, R_1 , of 60 mm, an outer radius, R_2 , of 135 mm, and is made from ASTM A723 steel with yield strength of 1100 MPa. During manufacture, the tube was overstrained to the extent that plastic deformation proceeded 50% through the tube wall thickness. Near the tube bore, the compressive residual stresses in the circumferential direction produced by the 50% overstrain are about half of the material yield strength, (Parker and Underwood, 1998). These residual stresses may have an important effect on the observed crack arrays, discussed in upcoming sections. The tube has a 0.12 mm thick layer of electro-deposited chromium on its inner surface which also plays an integral role in the crack arrays. The tube experienced forty prototype firings with a maximum propellant combustion gas temperature estimated to be 3550°C. The thermal damage and cracking observed near the tube bore are discussed next, with details of the temperature distribution in the tube wall in an upcoming section.

Figure 1 shows two metallographic sections of samples cut from the cannon tube at the same location. These sections show both the general configuration of the near-bore region of the tube and many of the details of the thermal and cracking damage that occurred as a result of firing. The 0.12 mm thick chromium layer (at the top of the photos) has a similar array of cracks in two orientations, with cracks normal to both the circumferential direction, Fig. 1[a], and axial direction, Fig. 1[b]. The cracks in the chromium often extend into the steel, and those that do are the dominant cracks of primary interest. Of particular interest is the observation that dominant L-R orientation cracks, Fig. 1[b], (in the plane normal to the longitudinal direction, extending in the radial direction) extend significantly further into the steel than do the dominant C-R cracks, Fig. 1[a]. The cracks in the Fig. 1 photos show this difference in depth, and the difference was found consistently in several other locations, as summarized in Table 1. The L-R cracks were typically twice as deep as C-R cracks, and the spacing of L-R cracks was more than three times that of C-R cracks. These differences may relate to the cause of cracking, so they beg investigation, particularly considering the facts that the deeper cracks are normal to the longitudinal direction which has no applied stress and the shallower cracks are normal to the circumferential direction which has significant tensile applied stress. This indicates that applied stresses do not control the observed cracking as is usually the case with cannons and other pressure vessels. The prime candidates for such control appear to be the residual stresses or some anisotropic behaviour of the material.

Other features to note in Fig. 1 are the following: [i] Evidence of a thermally induced transformation of steel at an average depth of 0.19 mm is particularly clear in Fig. 1(a), whose sample was etched to reveal the steel microstructure. The transformation from austenite to martensite occurs at about 750°C for the low alloy steel of interest here (Thornton and Colangelo, 1985). [ii] Indications of recrystallization of chromium at an average depth of 0.08 mm can be seen in Fig. 1(b), whose sample was etched to reveal the chromium microstructure. Chromium is quite noble, so the indications are not strong, but they are clear in the original photograph. The recrystallization of chromium was found by Marcinkowski (1959) to be complete at 1050°C.

TABLE 1 - Observations from metallographic sections of a fired cannon

| Depth of Chrome Recrystallization | Depth of Steel Transformation |
|------------------------------------|------------------------------------|
| 0.08 mm | 0.19 mm |
| Depth and Spacing of C-R Cracks | Depth and Spacing of L-R Cracks |
| depth: 0.23 mm spacing: 0.24 mm | depth: 0.46 mm spacing: 0.80 mm |

The microhardness indications in Fig 1(a) give further evidence of recrystallization; note that the chromium is softer than the unaffected steel, whereas as-plated chromium is known to be significantly harder than 1100 MPa yield strength steel. Thus it appears that the chromium has softened due to recrystallization.

Consequences of the thermal damage and cracking in the near-bore region of the tube are shown in Fig. 2. The overall damage process is the following. Cracks in the steel under the chromium link up, undermine and remove a section of chromium, and leave an area of direct contact between hot combustion gasses and steel. The lower melting temperature of steel combined with greatly increased convective heating near the missing section of chromium cause very rapid erosion pits and grooves, as shown in Fig. 2. The rapid erosion ruins the cannon tube, both by decreasing the fatigue life as considered in prior work (Underwood and Parker, 1995), and by affecting the projectile trajectory and velocity.

These observations are used in upcoming sections to develop a predictive model of near-bore thermal damage and cracking. In particular, the characteristic depths of the steel transformation and chromium recrystallization and the depths and spacing of the two different crack arrays are used to develop and confirm a thermomechanical model of near-bore damage that can be used to avoid some the severe consequences of firing damage in cannons.

NEAR-BORE TEMPERATURES

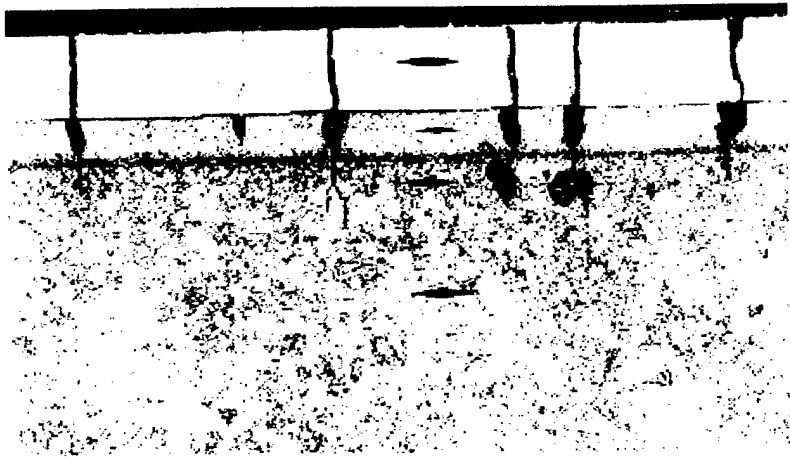
There is clear evidence that the nature of cracking during the first few firings of a gun tube is independent of local surface geometry. In prior results from the literature for a rifled gun tube the depth and spacing of cracking is the same in the land (the protruding sector of the rifling which imparts spin to the projectile) and its neighboring groove, (Gough and Morrison, 1984). In the case here, with no rifling, the crack depth and spacing are at least two orders of magnitude smaller than the wall thickness. It is therefore appropriate to model the materials as being of flat, semi-infinite extent, Fig. 3, consisting of a surface layer of chromium 0.12mm thick attached to a semi-infinite plate of steel.

During firing heat is applied for a brief period and is transmitted to the metals by a convective mechanism. Employing a standard analysis, (Incropera and DeWitt, 1985), the governing partial differential equation, based upon a single spatial coordinate, is:

$$\frac{\partial^2 T}{\partial x^2} = \frac{1}{\alpha} \frac{\partial T}{\partial t} \quad (1)$$

Circumferential
Stress
←-----→

(a)



Longitudinal
Stress
←-----→

(b)

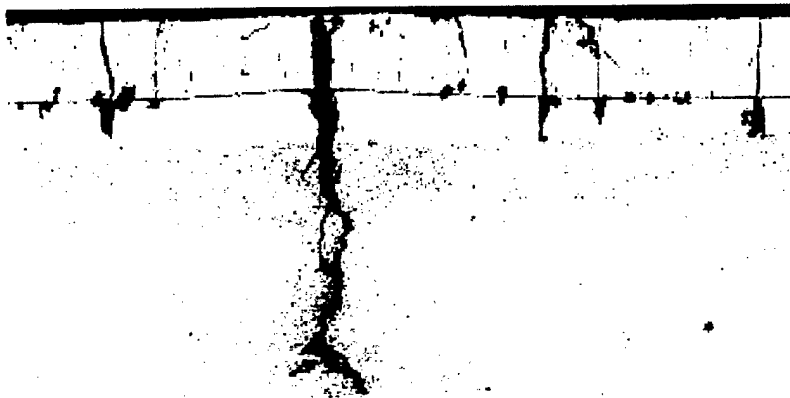


Figure 1 : Polished and Etched Sections from Near-Bore Region of a Cannon Following Forty Prototype Firings, 100X; (a) section showing C-R cracks, the steel microstructure and microhardness indentations; (b) section showing L-R cracks and the chromium microstructure.

Circumferential
Stress
←-----→



Figure 2 : Polished and Etched Sections from Near-Bore Region of a Cannon Following Forty Prototype Firings, 100X; section showing C-R cracks, the steel microstructure and the start of rapid erosion.

where T is absolute temperature, t is time, α is thermal diffusivity and x is the distance from the free surface.

The above equation may be solved analytically for a certain set of problems, and numerically for others. Solution of equation (1) requires an initial condition and two boundary conditions. Examples of analytical solutions for three cases are given in section 5.7 of Incropea and DeWitt (1985).

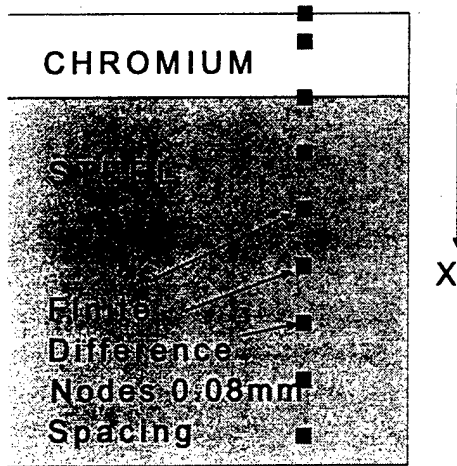


Figure 3 : Semi-Infinite Plate Representation and Location of Finite Difference Nodes

The important physical properties of the various media are: k , thermal conductivity (W/m.K); h , convection heat transfer coefficient (W/m².K); c_p , specific heat at constant pressure (J/kg.K) and α , thermal diffusivity (m²/second) where $\alpha = k/c_p$.

Equation (1) permits use of the explicit finite difference method via central-difference approximations, see Incropea and DeWitt (1985), section 5.9. This requires discretization in space (Δx) and in time (Δt) such that the stability criterion for the case of a single spatial dimension with a free surface is satisfied, namely:

$$\frac{\alpha \Delta t}{(\Delta x)^2} \left[1 + \frac{h \Delta x}{k} \right] \leq \frac{1}{2} \quad (2)$$

Numerical results presented herein were obtained using the above procedure. Typically $\Delta x = 0.04$ mm (surface), 0.08mm (elsewhere) and $\Delta t = 0.0001$ seconds with up to 25 nodes and 300 timesteps. The procedure incorporated material properties in both chromium and steel and permitted variation of such properties with temperature. Material properties and their variation with temperature are presented in Table 2. These represent best available information from Incropea and DeWitt (1985) and Dunn et al. (1995), but significant variations in the properties produced relatively minor shifts in derived maximum temperature profiles.

TABLE 2 : Thermal Properties of Metallic Materials Used in Finite Difference Procedure (T in Degrees Centigrade)

| | |
|------------|---|
| STEEL : | $k = 34.0$ $\alpha = 2.85E-6T^2 - 7.03E-3T + 9.89$ |
| CHROMIUM : | $k = 1.26E-5T^2 - 4.75E-2T + 94.4$ $\alpha = 6.72E-6T^2 - 2.40E-2T + 29.3$ |

The crucial unknown parameter is h , the convection heat transfer coefficient; $h = 0$ is equivalent to perfect insulation, $h = \infty$ is equivalent to full transfer of the maximum convective fluid temperature at the free surface. The range of h for gun tubes is potentially extremely large, (Fisher, 1996). h values in the range 10^5 to 10^6 W/m².K are indicated. The usual procedure for determination of an average, usable h value is a detailed thermo-fluids analysis, Dunn et al. (1995), and cross-correlation by experimental verification which normally involves the positioning of thermocouples as close as possible to the bore surface. This procedure, which involves drilling holes through the wall is difficult and can, in itself, potentially produce fluctuations which affect the desired measurements.

In order to circumvent such complexities and to obtain h values which are immediately usable, the experimental micrograph data, Figs. 1 and 2, were used. As mentioned previously, there is clear evidence of a transformation which extends to a total of 0.19mm below the free surface, i.e. 0.07mm below the chromium. Such a phase change occurs at a temperature of about 750°C and the boundary therefore indicates the maximum extent of the 750°C heating contour during the firing cycle.

This information together with the known maximum gas temperature (3550°C) and the gas temperature profile during the time of firing (0.015sec), (Sopok et al. (1997), makes it straightforward, iteratively, to solve for h such that the 750°C contour reaches the observed depth. Fig. 4 shows the Temperature-Time-Depth Profile; this indicates that a maximum temperature of 750°C is achieved at the required depth of 0.19mm with an h value of 198,000 W/m².K.

It is more useful, for subsequent analysis, to present the data of Fig. 4 in terms of maximum temperature versus depth. This is shown, for the case $h = 198,000$, as a single line in Fig. 5. Clearly it is a straightforward procedure to produce additional lines, each one relating to a different h value. Also shown in Fig. 5 are [i] the steel transformation point (750°C at 0.19mm depth) and the recrystallization point within the chromium (1050°C at 0.08mm depth) and [ii] inferred temperatures at the depth of maximum cracking for the C-R cracks and the L-R cracks using an accepted approximate stress intensity calculation described later.

NEAR-BORE THERMAL EXPANSION AND PHASE-CHANGE EFFECTS

The relationship between thermal expansion and phase changes for the steel under consideration should be straightforward, however within the literature there are examples of misunderstanding and of analytical predictions which do not match experimental evidence. It may therefore be of some value to list the major features and to point out a surprising result. Fig. 6 shows the results of detailed dilatometer

measurements by Cote and co-workers, reported in Thornton and Colangelo (1985), for the steel of concern.

a. During initial heating the steel expands linearly with temperature to point A. Over this range the coefficient of thermal expansion is the familiar one for steel, namely $12 \times 10^{-6}/^{\circ}\text{C}$.

b. At point A the phase-change to Austenite begins and the material contracts to point B, whereupon it resumes its expansion with temperature at a higher coefficient of thermal expansion. (Note: For firing of a cannon the full cycling of *all* material from A to B only occurs after a given number of thermal cycles. However for the purposes of this analysis it is sufficient to assume that such behavior is established.

c. During cooling the steel contracts at the higher rate until it reaches M_s , the Martensite transition temperature.

Note the following significant details:

- ◆ The Austenite phase change commences at 750°C and is complete at 790°C ,
- ◆ The increase in length between A and C (880°C) is less than or equal to zero,
- ◆ The change in length for the complete cycle 0 - A - B - C (and beyond) - M_s - 0 is zero
- ◆ The change in length between points A and B and between M_s and 0 is much less than the predicted 1.4% resulting from an analysis based upon changes in lattice parameters, (Reed-Hill, 1964). However Cote's results are supported by independent experimental studies of a similar low-alloy steel, (Hehmann, 1968).

NEAR-BORE STRESSES

In predicting the near-bore residual stresses resulting from the heating and cooling process it may be necessary to account for a variety of effects, e.g. :

- ◆ The initial residual stresses prior to heating (autofrettage including Bauschinger Effect)
- ◆ The compressive stresses produced by the thermal profile
- ◆ The onset and extent of compressive yielding due to thermal loading
- ◆ The tensile contribution on cooling
- ◆ The contribution of phase-change effects to stresses during heating and cooling
- ◆ The possibility of yielding in tension together with the impact of subsequent crack development upon such yielding during subsequent firing cycles
- ◆ The possibility that residual stresses produced in the chromium during plating will affect the stresses in the adjacent steel and its cracking behavior

Potentially the above interactions are extremely complex. To permit further analysis we make the following pragmatic assumptions:

a. That for a tube which has undergone more than 40% autofrettage there is already reversed yielding in compression at the bore as a result of the Bauschinger effect. This extends throughout the region of interest at a level of 0.38 times uniaxial yield strength for the hoop direction which in turn generate 0.114 (i.e. $0.38 \times$ Poisson's ratio) times uniaxial yield strength for the axial direction.

b. That the yield strength of the material in compression resulting from near-bore high temperatures will be a function of those temperatures and should be taken into account in assessing the onset of compressive yielding if it is of smaller magnitude than the Bauschinger affected yield strength.

c. That the cooling process produces biaxial tensile stresses at near-bore locations which can be superimposed elastically upon those in (a) and/or (b). These stresses are given by

$$\sigma(x) = [E\alpha * \Delta T(x)]/[1 - \nu] \quad (3)$$

where α^* is coefficient of thermal expansion in $\text{m/m} \cdot ^{\circ}\text{C}$, ν is Poisson's ratio and the $[1-\nu]$ term arises from the biaxial nature of the thermal field.

Thus far the temperature-profile calculations have differentiated between properties of steel and chromium. In the stress calculations steel properties are assumed for the chromium layer. For a variety of reasons this assumption is unlikely to influence the desired stress intensity calculations for cracks within the steel. The reasons include; the intense, multiple pre-cracked nature of the chromium and the sensitivity of the stress intensity calculations to stress at prospective crack tip location (within the steel) and of crack spacing rather than crack depth.

Fig. 7 shows these predicted residual stress profiles for hoop and axial directions. The curve which increases monotonically to the bore ignores phase-change effects. Phase-change effects can be approximated based on the fact (in Fig. 5) that none of the steel exceeds 880°C at any time. Thus the maximum change in length will be that associated with 750°C within the range 750°C to 880°C , Fig. 6. This serves to limit the resulting residual stresses as shown in Fig. 7.

No attempt has been made to limit residual tensile stresses at the yield strength value. There are two reasons for this decision. First the subsequent calculation of stress intensity, dominated as it is by stress at the prospective location of the crack tip, is relatively insensitive to the very-near-bore stresses that may exceed yield. Second, as cracks appear they serve to reduce the constraint in the very-near-bore region and thus reduce the extent of any yielding in tension.

The residual stresses taking account of phase-change limits shown in Fig. 7 were used to calculate the crack tip stress intensity factors, K , presented in Fig. 8. The method used to obtain K is of extremely high accuracy (errors $< 0.5\%$) and involves the modified mapping collocation technique, (Andrasic and Parker, 1984) packaged as weight function data (Andrasic and Parker, 1982). It is possible to apply approximate bounds to these solutions, (Parker, 1998), using the stress normal to the prospective crack line at the location of the prospective crack tip, σ^* . In the case of very short cracks $K = 1.12\sigma^* \sqrt{\pi a}$ where a is crack depth, whereas when the cracks are much deeper $K = \sigma^* \sqrt{d}$ where $2d$ is the crack spacing. This latter form was used to obtain the approximate temperatures for each of the crack depths presented in Fig. 5. However it is necessary to repeat the caveat in Parker (1998); this approximation may not be sufficiently accurate in regions of high stress gradients as occurs in this case.

Two curves are shown in Fig. 8, [i] that relating to the deepest (L-R) cracks, spacing 0.8mm [ii] that relating to the shallower (C-R) cracks, spacing 0.24mm. A typically observed threshold for the

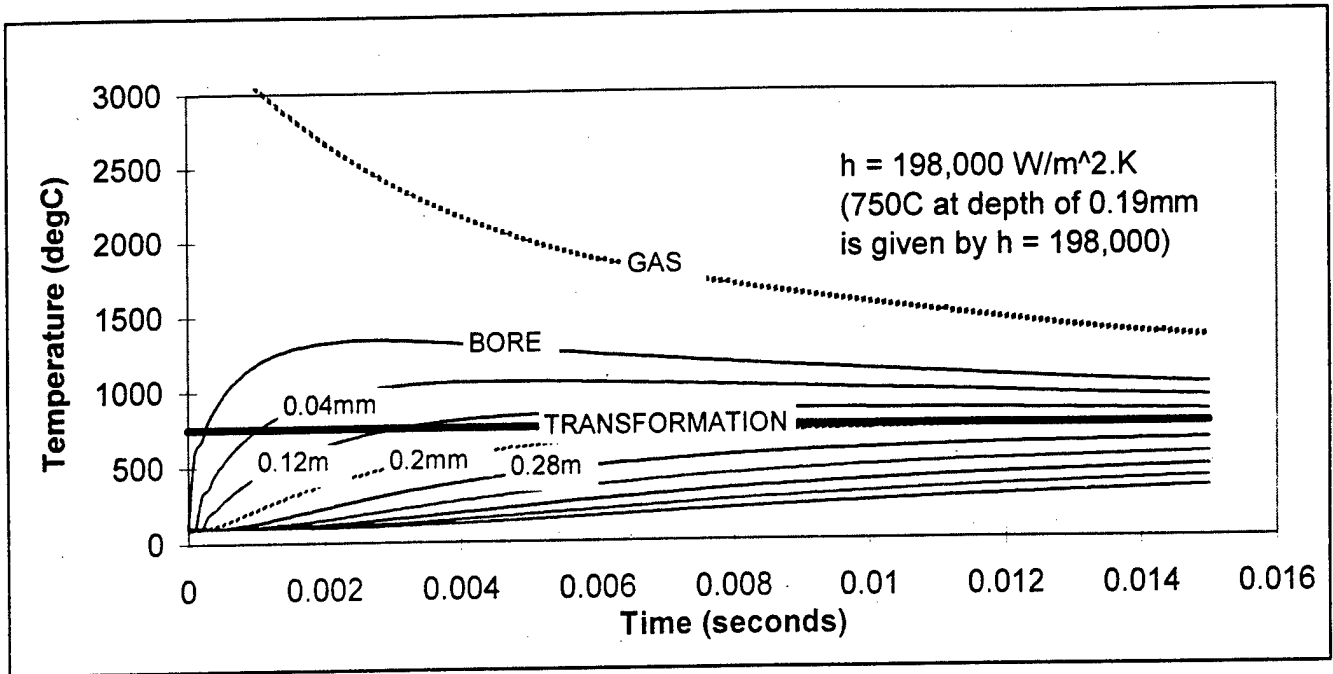


Fig. 4 : Finite Difference Temperature-Time-Depth Profile Based Upon Known Depth of Transformation.

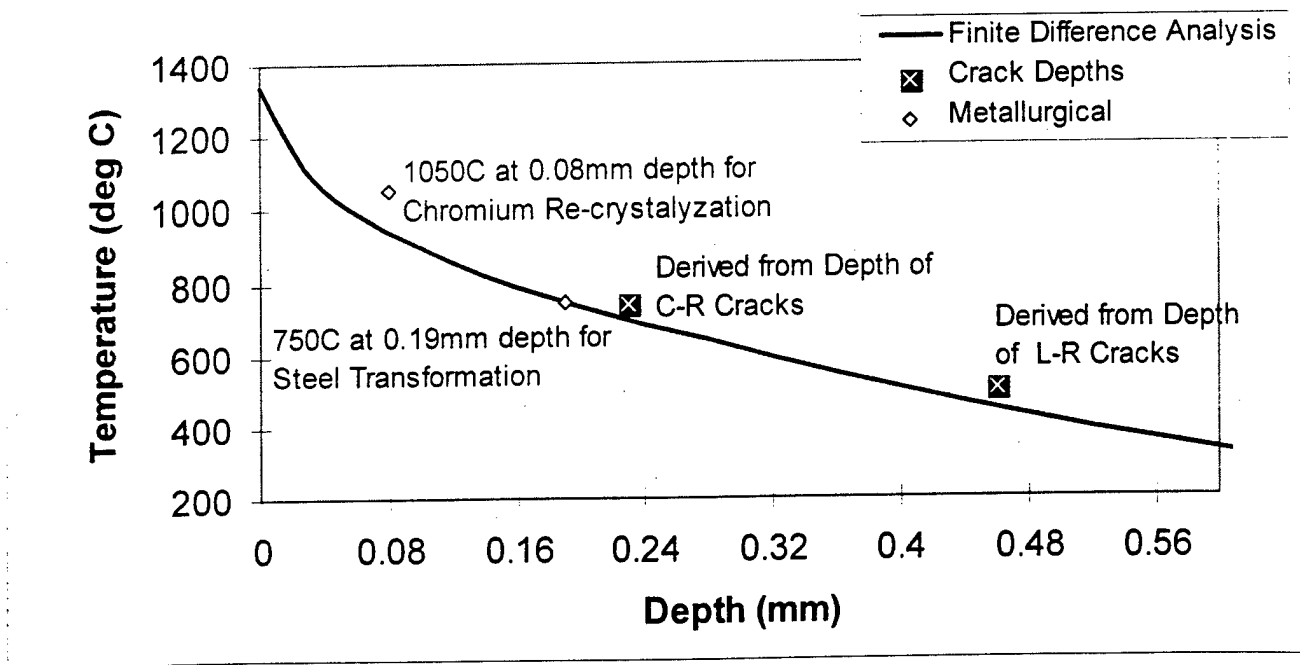


Fig. 5 : Finite Difference Maximum Temperature versus Depth for $h = 198,000 \text{ W/m}^2.K$

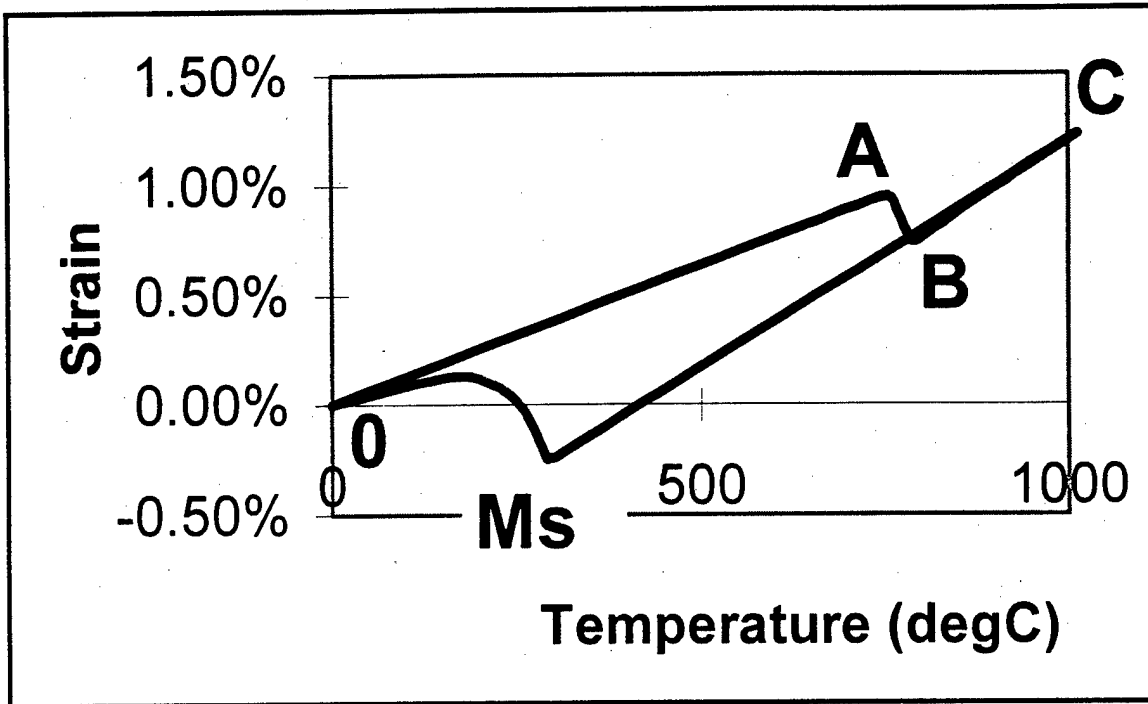


Figure 6: Dilation Behavior of a Low Alloy Steel as a Function of Temperature

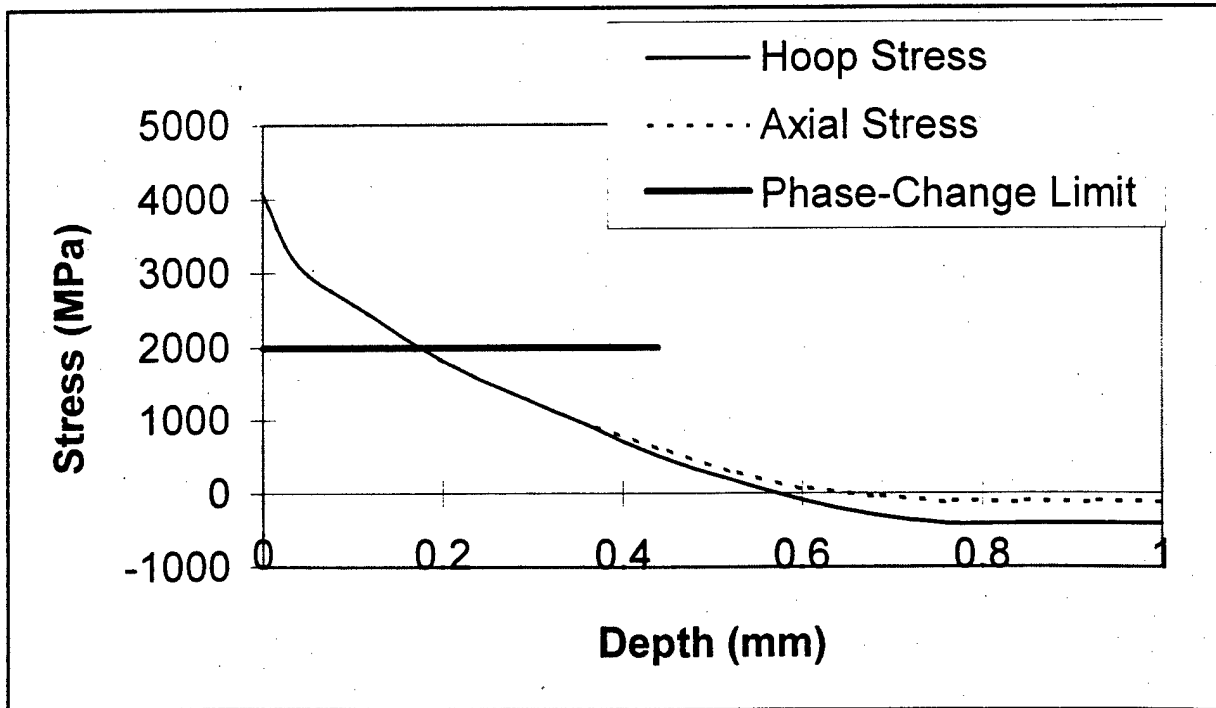


Figure 7: Near-Bore Residual Stresses After Heating and Cooling

relatively rapid hydrogen cracking observed in cannon tubes, 23 MPam^{3/2}, (Vigilante et al., 1997) is shown as a horizontal line.

plastic strain in the relevant planes which may influence stress corrosion cracking rate and/or threshold value.

SUMMARY AND CONCLUSIONS

Results from Analysis

The stress intensity calculations relating to the two observed spacings for C-R and L-R cracks shown in Fig. 8 provide convincing indications that the observed depth of cracking is related closely to a KSCC threshold value of around 23 MPam^{3/2} and this value, in turn, is consistent with experimental observations of Vigilante et al. (1997).

Less obvious is the reason why the L-R cracks, which initially followed an almost identical K versus depth profile to the C-R cracks, 'elected' to increase their spacing, and hence their K values, to follow the upper (L-R) curve of Fig. 8. Inspection of Fig. 7 which shows the autofrettage stress field into which the cracks are proceeding, indicates that the C-R cracks are moving towards a more compressive stress regime. However, this effect is subtle at the depths of interest here and may not provide a complete explanation.

In recent work, still under way, it has been noted that the magnitude of prior plastic strain on the two planes of interest here is strongly influenced by the autofrettage process itself, whether hydraulic or swage. Thus another, possibly complementary, explanation for the differential crack depths is the amount of prior

Cause and Prevention of Cracking

The nature of the observed cracking (Figs. 1-2), combined with our experience of hydrogen cracking in cannon subjected to somewhat similar firing conditions (Sopok et al., 1997; Vigilante et al., 1997), indicated that hydrogen cracking had indeed occurred in this cannon tube. Of the three broadly accepted requirements for environmental cracking - an aggressive environment, a susceptible material, and a sustained tensile stress - the former two elements must be considered to be always present in cannon firing. Hydrogen is generally present in cannon propellant combustion gasses, and 1100MPa yield strength A723 steel is clearly susceptible to hydrogen cracking (Sopok et al., 1997; Vigilante et al., 1997). Therefore the cause of cracking here must be related to a significantly increased presence of sustained tensile stress, as explained by the results summarized in Figs. 5 and 7. The calculated near-bore temperatures, in agreement with metallurgical and cracking evidence (Fig. 4), produce compressive yielding and resultant tensile residual stresses well below the 0.12mm depth of the chromium layer (Fig. 7). These tensile stresses, at significantly greater depth and higher magnitude than in prior cannon firing experience, are the cause of the hydrogen cracking.

Prevention of this type of hydrogen cracking in cannon is not easy, considering the accepted requirements for cracking discussed earlier. Elimination of the hydrogen environment or replacement of the A723

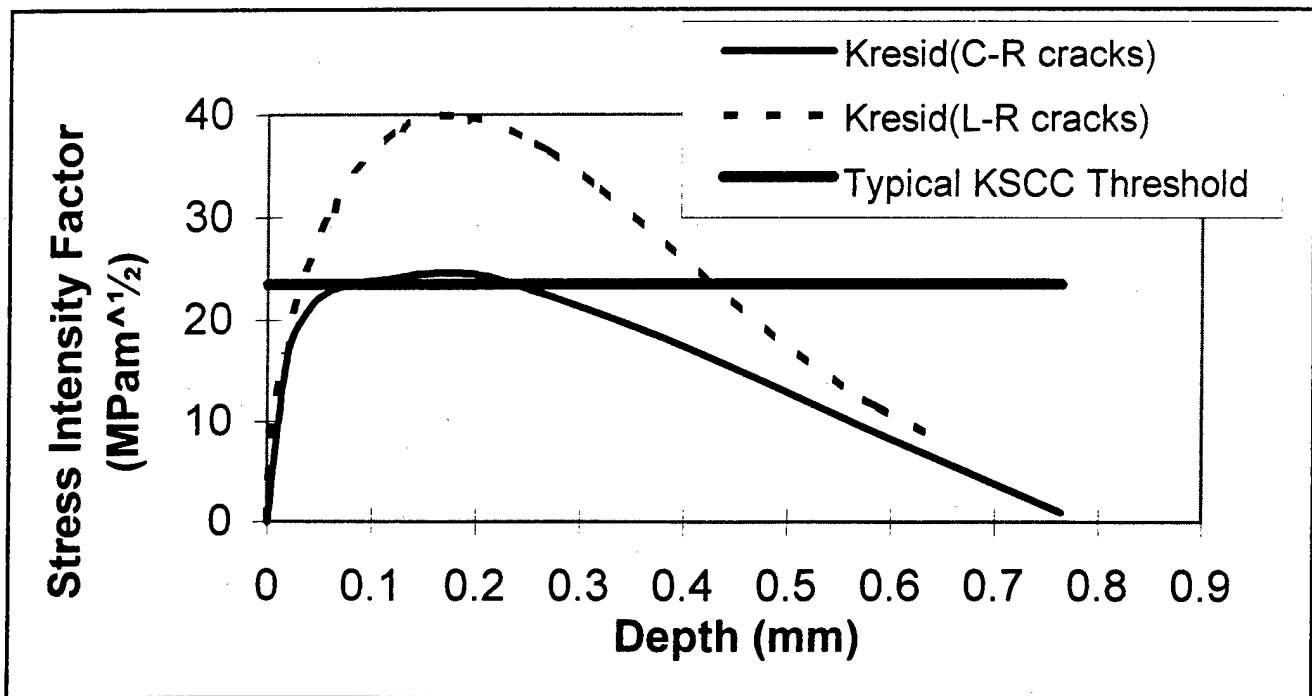


Figure 8: Stress Intensity Factors for C-R and L-R Cracks Based Upon Observed Crack Spacing

steel would be a major design change, and reducing the firing temperature affects cannon function, as discussed earlier. Two types of preventative measure that have some promise are [i] providing an improved physical and chemical barrier to the hydrogen, or [ii] providing an improved thermal barrier to the hot gasses. An interlayer of electrodeposited nickel between the chromium and steel would be an effective hydrogen barrier and is under investigation by the present authors. A coating of increased thickness or decreased thermal conductivity would improve the thermal barrier and thereby reduce the level of tensile residual stress that causes cracking.

ACKNOWLEDGEMENTS

Much of this work was undertaken during an attachment by one of the authors (APP) to the US Army Armament Research, Development and Engineering Center (ARDEC), Watervliet, NY. The attachment was arranged via the European Research Office of the US Army Research, Development and Standardization Group (UK). The authors gratefully acknowledge valuable discussions with Mr. P. O'Hara and Mr. J. Cox of ARDEC.

REFERENCES

- Andrasic, C. P. and Parker, A. P., 1982, "Spline Fit Weight Function Data for Cracked Thick Cylinders", Royal Military College of Science Technical Note MAT/36, Shrivenham, England.
- Andrasic, C. P., and Parker, A. P., 1984, "Dimensionless Stress Intensity Factors for Cracked Thick Cylinders Under Polynomial Crack Face Loadings", *Engng Frac Mech*, Vol 19, 1, pp. 187-193.
- Dunn, S., Sopok, S., Coats, D., O'Hara, P., Nickerson, G. and Pfligl, G., 1995, "Unified Computer Model for Predicting Thermochemical Erosion in Gun Barrels", US Army ARDEC, Benét Laboratories, ARCCB-TR-95030.
- Fisher, E. B., 1996, "Gun Barrel Heating and Wear Environment", Proceedings of 42nd Sagamore Workshop on Gun Barrel Wear and Erosion, DuPont Country Club, Wilmington, DE, 29-31 July 1996, pp591-611. Published by US Army, Aberdeen Proving Ground, Maryland.
- Gough, J.P., and Morrison, J., 1984, "Craze Cracking in 105mm Artillery and Tank Gun Barrels", Canadian Defence Research Establishment Pacific, Technical Memorandum 84-9.
- Hehmann, R. F., 1968, "The Bainite Transformation", in Chapter 9 of *Phase Transformations*, American Society for Metals, Metals Park, OH.
- Incropera, F. P., and DeWitt, D. P., 1985, *Introduction to Heat Transfer*, Wiley, New York, pp. 259-263.
- Marcinkowski, M. J., 1959, "Plastic Deformation of Chromium at Low Temperatures", Aeronautical Research Laboratory, Wright-Patterson AFB, WADC TR 50-294; (AD2116260).
- Parker, A. P., 1998, "Stability of Arrays of Multiple Edge Cracks", Army Armament RD&E Center, Watervliet Technical Report (in preparation). To be submitted to *Engng Frac Mech*.
- Parker, A. P. and Underwood, J. H., 1998, "Influence of Bauschinger Effect on Residual Stress and Fatigue Lifetimes in Autofrettagged Thick Walled Cylinders", *Fatigue and Fracture Mechanics: 29th Volume, ASTM STP 1321*, T. L. Panontin and S. D. Sheppard, Eds., American Society for Testing and Materials. (In press)
- Reed-Hill, R. E., 1964, *Physical Metallurgy Principles*, Van Nostrand, pp503-504.
- Sopok, S., O'Hara, P., Vottis, P., Pfligl, G., Rickard, C. and Loomis, R., 1997, "Erosion Modeling of the 120-MM M256.M829A2 Gun System", Army Armament RD&E Center, Watervliet, ARCCB-TR-97011, 1997, presented at 1997 ADPA Gun and Ammunition Symposium, San Diego, 7-10 April 1997.
- Thornton, P. A. and Colangelo, V. J., 1985, *Fundamentals of Engineering Materials*, Prentice Hall, p. 419 Fig. 12-18 (courtesy P. J. Cote).
- Underwood, J. H., and Parker, A. P., 1995, "Fatigue Life Analyses and Tests for Thick-Wall Cylinders Including Effects of Overstrain and Axial Grooves", *Journal of Pressure Vessel Technology*, Vol. 117, pp. 222-226.
- Vigilante, G. N., Underwood, J. H., Crayon, D., Tauscher, S., Sage, T. and Troiano, E., 1997, "Hydrogen Induced Cracking Tests of High Strength Steels and Nickel-Iron Base Alloys using the Bolt-Loaded Specimen", *Fatigue and Fracture Mechanics: 28th Volume, ASTM STP 1321*, American Society for Testing and Materials, pp 602-616.

TECHNICAL REPORT INTERNAL DISTRIBUTION LIST

| | <u>NO. OF COPIES</u> |
|---|--------------------------|
| CHIEF, DEVELOPMENT ENGINEERING DIVISION | |
| ATTN: AMSTA-AR-CCB-DA | 1 |
| -DB | 1 |
| -DC | 1 |
| -DD | 1 |
| -DE | 1 |
| CHIEF, ENGINEERING DIVISION | |
| ATTN: AMSTA-AR-CCB-E | 1 |
| -EA | 1 |
| -EB | 1 |
| -EC | 1 |
| CHIEF, TECHNOLOGY DIVISION | |
| ATTN: AMSTA-AR-CCB-T | 2 |
| -TA | 1 |
| -TB | 1 |
| -TC | 1 |
| TECHNICAL LIBRARY | |
| ATTN: AMSTA-AR-CCB-O | 5 |
| TECHNICAL PUBLICATIONS & EDITING SECTION | |
| ATTN: AMSTA-AR-CCB-O | 3 |
| OPERATIONS DIRECTORATE | |
| ATTN: SIOWV-ODP-P | 1 |
| DIRECTOR, PROCUREMENT & CONTRACTING DIRECTORATE | |
| ATTN: SIOWV-PP | 1 |
| DIRECTOR, PRODUCT ASSURANCE & TEST DIRECTORATE | |
| ATTN: SIOWV-QA | 1 |

NOTE: PLEASE NOTIFY DIRECTOR, BENÉT LABORATORIES, ATTN: AMSTA-AR-CCB-O OF ADDRESS CHANGES.

TECHNICAL REPORT EXTERNAL DISTRIBUTION LIST

| | <u>NO. OF COPIES</u> | | <u>NO. OF COPIES</u> |
|---|---------------------------------|--|--------------------------|
| ASST SEC OF THE ARMY RESEARCH AND DEVELOPMENT ATTN: DEPT FOR SCI AND TECH THE PENTAGON WASHINGTON, D.C. 20310-0103 | 1 | COMMANDER ROCK ISLAND ARSENAL ATTN: SMCRI-SEM ROCK ISLAND, IL 61299-5001 | 1 |
| DEFENSE TECHNICAL INFO CENTER ATTN: DTIC-OC (ACQUISITIONS) 8725 JOHN J. KINGMAN ROAD STE 0944 FT. BELVOIR, VA 22060-6218 | 2 | COMMANDER U.S. ARMY TANK-AUTMV R&D COMMAND ATTN: AMSTA-DDL (TECH LIBRARY) WARREN, MI 48397-5000 | 1 |
| COMMANDER U.S. ARMY ARDEC ATTN: AMSTA-AR-AEE, BLDG. 3022 AMSTA-AR-AES, BLDG. 321 AMSTA-AR-AET-O, BLDG. 183 AMSTA-AR-FSA, BLDG. 354 AMSTA-AR-FSM-E AMSTA-AR-FSS-D, BLDG. 94 AMSTA-AR-IMC, BLDG. 59 PICATINNY ARSENAL, NJ 07806-5000 | 1 1 1 1 1 1 2 | COMMANDER U.S. MILITARY ACADEMY ATTN: DEPARTMENT OF MECHANICS WEST POINT, NY 10966-1792 U.S. ARMY MISSILE COMMAND REDSTONE SCIENTIFIC INFO CENTER ATTN: AMSMI-RD-CS-R/DOCUMENTS BLDG. 4484 REDSTONE ARSENAL, AL 35898-5241 | 1 2 |
| DIRECTOR U.S. ARMY RESEARCH LABORATORY ATTN: AMSRL-DD-T, BLDG. 305 ABERDEEN PROVING GROUND, MD 21005-5066 | 1 | COMMANDER U.S. ARMY FOREIGN SCI & TECH CENTER ATTN: DRXST-SD 220 7TH STREET, N.E. CHARLOTTESVILLE, VA 22901 | 1 |
| DIRECTOR U.S. ARMY RESEARCH LABORATORY ATTN: AMSRL-WT-PD (DR. B. BURNS) ABERDEEN PROVING GROUND, MD 21005-5066 | 1 | COMMANDER U.S. ARMY LABCOM, ISA ATTN: SLCIS-IM-TL 2800 POWER MILL ROAD ADELPHI, MD 20783-1145 | 1 |

NOTE: PLEASE NOTIFY COMMANDER, ARMAMENT RESEARCH, DEVELOPMENT, AND ENGINEERING CENTER,
BENÉT LABORATORIES, CCAC, U.S. ARMY TANK-AUTOMOTIVE AND ARMAMENTS COMMAND,
AMSTA-AR-CCB-O, WATERVLIET, NY 12189-4050 OF ADDRESS CHANGES.

TECHNICAL REPORT EXTERNAL DISTRIBUTION LIST (CONT'D)

| | <u>NO. OF COPIES</u> | | <u>NO. OF COPIES</u> |
|---|--------------------------|--|--------------------------|
| COMMANDER U.S. ARMY RESEARCH OFFICE ATTN: CHIEF, IPO P.O. BOX 12211 RESEARCH TRIANGLE PARK, NC 27709-2211 | 1 | WRIGHT LABORATORY ARMAMENT DIRECTORATE ATTN: WL/MNM EGLIN AFB, FL 32542-6810 | 1 |
| DIRECTOR U.S. NAVAL RESEARCH LABORATORY ATTN: MATERIALS SCI & TECH DIV WASHINGTON, D.C. 20375 | 1 | WRIGHT LABORATORY ARMAMENT DIRECTORATE ATTN: WL/MNMF EGLIN AFB, FL 32542-6810 | 1 |

NOTE: PLEASE NOTIFY COMMANDER, ARMAMENT RESEARCH, DEVELOPMENT, AND ENGINEERING CENTER,
BENÉT LABORATORIES, CCAC, U.S. ARMY TANK-AUTOMOTIVE AND ARMAMENTS COMMAND,
AMSTA-AR-CCB-O, WATERVLIET, NY 12189-4050 OF ADDRESS CHANGES.
